Rearrangement of Chorismate to Prephenate. Use of Chorismate Mutase Inhibitors to Define the Transition State Structure†

P. R. Andrews,*,‡ E. N. Cain,§ E. Rizzardo,¶ and G. D. Smith

ABSTRACT: The enzymically catalyzed conversion of chorismate to prephenate may proceed through either a chair-like or a boat-like transition state. To distinguish between these alternatives, we have prepared a series of structural analogues of the two possible transition state structures and tested them as inhibitors of chorismate mutase–prephenate dehydrogenase from *Escherichia coli* K12. The results indicate that the enzymically catalyzed reaction passes through a chair-like intermediate. None of the compounds studied is an ideal transition state analogue; it seems likely that the partial bond structure of the transition state precludes the corresponding orientation of the side chain in stable molecules. Nevertheless, the new inhibitors are stronger than any previously available, and the degree of inhibition is consistent with bacteriostatic activity recently observed in some of the compounds.

The isomerization of chorismate to prephenate (Figure 1) is the first specific step in the biosynthetic pathways leading to tyrosine and phenylalanine in bacteria and other organisms (Gibson and Pittard, 1968). The reaction is an oxy-Cope rearrangement catalyzed by either chorismate mutase–prephenate dehydrogenase (EC 1.3.1.12) or chorismate mutase–prephenate dehydratase (EC 4.2.1.51); it also proceeds nonenzymatically (Andrews et al., 1973).

In general, Cope rearrangements are known to pass through a chair-like arrangement of the transition state, this being favored by at least 5 kcal/mol over the alternative boat conformation (Doering and Roth, 1962). Molecular orbital calculations using the MINDO/3 method confirm, both qualitatively and quantitatively, this preference for the chair pathway in geometrically unrestricted Cope rearrangements (Dewar, 1975). In the present example, however, both extended Hückel (Andrews et al., 1973) and MINDO/3 (Andrews and Haddon, in preparation) calculations show that the chair form is favored by less than 2 kcal/mol. The transition state stabilization required for catalysis via the chair pathway is therefore not much less than that needed to account for catalysis via the boat pathway, and the enzyme-catalyzed reaction could pass through either intermediate. In principle, the actual pathway could be deduced from the stereochemistry of the products obtained from stereospecifically labelled chorismate, but efforts to prepare the starting material have not been successful (Ife et al., 1976). Instead, we have attempted to solve the problem by designing structural analogues for both of the possible transition state conformations, and testing them as inhibitors of chorismate mutase–prephenate dehydrogenase from *E. coli*. The rationale behind our approach is that inhibitors resembling the true transition state will produce the strong inhibition characteristic of transition state analogues (Wolfenden, 1976), whereas those resembling the alternative transition state will not. We also note that potent inhibitors of the enzyme, which occurs in bacteria and plants but not in man, may have potential as antibiotics and/or herbicides.

Experimental Section

Adamantane-1,3-dicarboxylic acid and 6-hydroxyadamantane-1,3-dicarboxylic acid were synthesized from diethyl 2,6-dioxoadamantane-1,3-dicarboxylate, and the structure of the latter product was established by spectral examination and microanalysis of both the diacid and its dimethyl ester (Cain and Welling, 1975). 1-Carboxyadamantane-3-acetic acid was prepared by treating 1-bromoadamantane-3-acetic acid (Bott, 1968) with formic acid in concentrated sulfuric acid (Stetter et al., 1959). The four geometric isomers of 6-hydroxybicyclo[3.3.1]nonane-1,3-dicarboxylic acid were synthesized from tetramethyl 2,6-dioxobicyclo[3.3.1]nonane-1,3,5,7-tetracarboxylic acid (Schaefer and Honig, 1968) via 6-oxobicyclo[3.3.1]non-2-ene-1,3-dicarboxylic acid. Reduction of the latter with Raney nickel under equilibrating conditions (Marvell and Knutson, 1970) yielded a mixture of *endo*-6-hydroxybicyclo[3.3.1]nonane-1,*endo*-3-dicarboxylic acid and *exo*-6-hydroxybicyclo[3.3.1]nonane-1,*endo*-3-dicarboxylic acid. These were separated by gas–liquid chromatography as the dimethyl esters–Me_3Si ethers and each one was epimerized at carbon 3 with sodium methoxide (Appleton et al., 1968), to give the remaining isomers: *endo*-6-hydroxybicyclo[3.3.1]-nonane-1,*exo*-3-dicarboxylic acid and *exo*-6-hydroxybicyclo[3.3.1]nonane-1,*exo*-3-dicarboxylic acid. Each of the four geometric isomers is a racemic mixture of two enantiomers but further resolution was not attempted. The ring conformations expected on the basis of steric considerations were confirmed by nuclear magnetic resonance. The hydroxyl containing ring is chair in all cases, while the 3-carboxyl containing ring is chair in the exo isomers and boat in the endo forms. Details of the synthesis, characterization, and conformation of these isomers will be published elsewhere (Rizzardo, in preparation).

Adamantane-1-acetic acid, adamantane-1-carboxylic acid, 1-aminoadamantane, 1-hydroxyadamantane, and adamantane-1,3-diacetic acid were purchased from Aldrich Chemical Co. Chorismate was kindly donated by Dr. I. G. Young.

Chorismate mutase–prephenate dehydrogenase was prepared by the method of Koch et al. (1971) and stored at −12

†From the Department of Physical Biochemistry, John Curtin School of Medical Research, the Department of Biochemistry, Faculty of Science, and the Research School of Chemistry, Australian National University, Canberra, A.C.T. 2601, Australia. *Received May 23, 1977.*

‡Department of Physical Biochemistry, The John Curtin School of Medical Research, Australian National University, Canberra A.C.T. 2601, Australia.

§Australian Science and Technology Council (ASTEC), Canberra, A.C.T. 2600, Australia.

¶CSIRO Division of Applied Organic Chemistry, Fishermen's Bend, Melbourne, Victoria, 3001, Australia.

||Department of Biochemistry, Faculty of Science, Australian National University, Canberra, A.C.T. 2601, Australia.

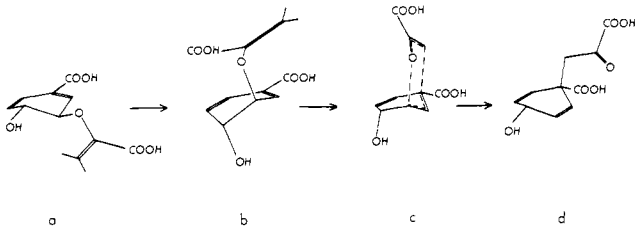

FIGURE 1: The isomerization of chorismate to prephenate; (a) chorismate (equatorial), (b) chorismate (axial), (c) transition state (chair conformation), and (d) prephenate. The molecules are shown in the lowest energy conformations obtained from molecular orbital calculations (Andrews et al., 1973).

°C in 30% glycerol in their buffer A. Its specific activity was 0.9 μmol min^{-1} (mg of protein)$^{-1}$. Chorismate mutase activity was measured spectrophotometrically by observing the disappearance of chorismate or by detecting the formation of prephenate after conversion to phenylpyruvate (Koch et al., 1971). Coupled assays were performed by observing the production of NADH from chorismate plus NAD (Koch et al., 1972). In cases where the buffer capacity was insufficient due to the presence of inhibitors, the pH was adjusted with NaOH.

To facilitate molecular comparisons, computer programs were written to superimpose stereoscopic displays of two or more molecular models. This was achieved by minimizing the sum of the distances between equivalent atoms with respect to the six degrees of intermolecular rotational and translational freedom as well as internal conformational variables.

Results

Previous work has suggested that chorismate mutase–prephenate dehydrogenase shows sigmoidal kinetics in its mutase activity (Koch et al., 1971). We have confirmed this (Figure 2), although we found a significantly lower apparent K_m value (0.11 mM); this was measured as the substrate concentration at half maximal velocity. Because of the sigmoidality we have chosen to describe the inhibition results in terms of apparent K_I values. These were obtained from plots of velocity vs. inhibitor concentration and represent half the concentration of inhibitor required to give 50% inhibition at a substrate concentration equal to the apparent K_m. In the analogous case of an enzyme exhibiting strictly Michaelis–Menten kinetics such a procedure would yield true K_I values. The results are given in Table I.

The strongest inhibitor, adamantane-1-acetic acid, was used for a more detailed study at higher substrate concentrations where the Lineweaver–Burk plots, which became essentially linear, demonstrated that inhibition is competitive.

In separate experiments using prephenate and NAD as substrates it was shown that adamantane-1-acetic acid was also an inhibitor of the dehydrogenase activity of the enzyme, but inhibition studies using the coupled assay method showed that this inhibitor produced no significant lag periods in the product vs. time plots (e.g., Figure 3). The overriding effect in this assay is therefore on the mutase activity. In contrast, inhibition by the final reaction product, 4-hydroxyphenylpyruvate, which preferentially inhibits the dehydrogenase reaction, resulted in a large increase in the lag time (Figure 3).

Discussion

Transition State Structure. The chair- and boat-like transition state structures are shown diagrammatically in Figures 4a and 5a, respectively. They illustrate two problems of transition state analogue design. First, the partial bonds in transition state structures give rise to bond lengths and hybridization states which cannot be reproduced in stable molecules. Second, the accumulation of chemical features in transition state structures may be incompatible with synthetic feasibility. Bearing these limitations in mind, we chose to synthesize *exo*-6-hydroxybicyclo[3.3.1]nonane-1-*exo*-3-dicarboxylic acid (Figure 4b) and *exo*-6-hydroxybicyclo[3.3.1]nonane-1-*endo*-3-dicarboxylic acid (Figure 5b) as the closest practicable analogues of the chair- and boat-like transition state structures, respectively. Although differing from each other only in their stereochemistry around a single carbon atom, they adopt the chair–chair and chair–boat conformations, respectively (see Experimental Section) and, thus, closely reproduce the topographical differences between the alternative transition state structures. The substantial inhibition of chorismate mutase by the *exo*-COOH nonane (Table I), but not by the *endo*-COOH isomer, therefore suggests that the enzymically cata-

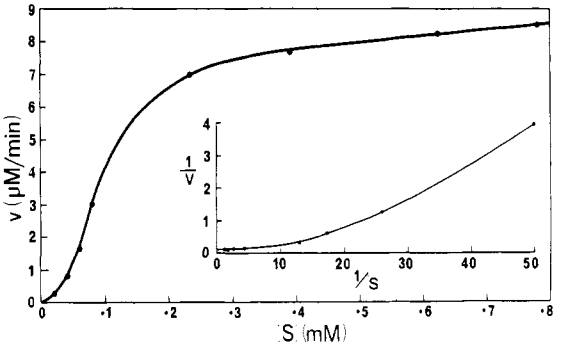

FIGURE 2: The variation of chorismate mutase activity, v, with chorismate concentration, [S], together with (insert) a double-reciprocal plot of $1/v$ vs. $1/[S]$.

TABLE I: Inhibition of Chorismate Mutase by Nonanes, Adamantanes, and Related Structures.

Inhibitor	K_I^{app} (M)[a]
6-Hydroxybicyclo[3.3.1]nonane-1,3-dicarboxylic acids[b]	
exo-Hydroxy-*exo*-3-carboxyl	3.9×10^{-4}
exo-Hydroxy-*endo*-3-carboxyl	*c*
endo-Hydroxy-*exo*-3-carboxyl	*d*
endo-Hydroxy-*endo*-3-carboxyl	*d*
Adamantanes	
6-Hydroxyadamantane-1,3-dicarboxylic acid	6.5×10^{-4}
Adamantane-1-carboxylic acid	1.5×10^{-4}
Adamantane-1-acetic acid	1.2×10^{-4}
1-Hydroxyadamantane	9.4×10^{-4}
1-Aminoadamantane	3.5×10^{-2}
Adamantane-1,3-dicarboxylic acid	5.5×10^{-3}
Adamantane-1,3-diacetic acid	6.2×10^{-4}
1-Carboxyadamantane-3-acetic acid	1.3×10^{-3}
Others	
Benzoic acid	2.0×10^{-3}
Phenylacetic acid	1.9×10^{-3}
Phenol	3.9×10^{-3}
Acetic acid	4.9×10^{-2}

[a] K_I^{app} is defined as half the inhibitor concentration giving 50% inhibition when the substrate concentration is set equal to K_m. [b] These compounds are racemic mixtures. The K_I^{app} for the appropriate isomer may therefore be as little as half the value given. [c] No inhibition was observed at 2.5×10^{-3} M. Higher concentrations were not tested because of the limited material available. [d] No inhibition was observed at 5.0×10^{-3} M. Higher concentrations were not tested because of the limited material available.

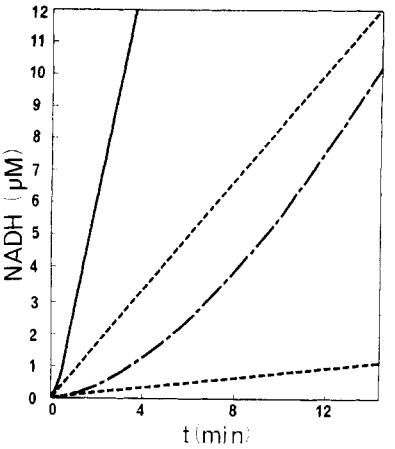

FIGURE 3: Product (NADH) vs. time plots obtained using coupled assays which measure the conversion of chorismate via prephenate to 4-hydroxyphenylpyruvate by chorismate mutase–prephenate dehydrogenase. A sample of enzyme was assayed with a chorismate concentration of 1.2 mM and NAD concentration of 0.2 mM in the absence (—) and presence of the inhibitors adamantane-1-acetic acid (- - - -) at 2.5 mM (upper line) and 4.1 mM (lower line) and 4-hydroxyphenylpyruvate at 5.0 mM (— - — - —). The traces were recorded continuously on a recording spectrophotometer.

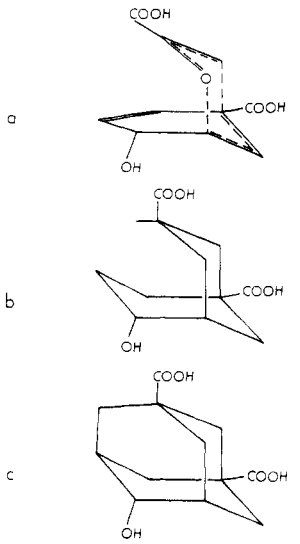

FIGURE 4: Diagrammatic representations of the chair-like alternative for the transition state structure and two proposed analogues of this conformation. (a) Chair-like transition state structure; (b) *exo*-6-hydroxybicyclo[3.3.1]nonane-1,*exo*-3-dicarboxylic acid; (c) 6-hydroxyadamantane-1,3-dicarboxylic acid.

lyzed reaction passes through a chair-like intermediate. The inhibition due to the *exo*-COOH nonane is not, however, as strong as expected for an ideal transition state analogue, and it could be argued that an energetically less favored, and consequently less populated, conformation of the nonane may produce the observed inhibition by substantially tighter binding. To test this possibility we prepared an additional analogue, 6-hydroxyadamantane-1,3-dicarboxylic acid (Figure 4c), in which the chair-chair conformation is fixed by the addition of a bridging methylene group. The observed K_I for this compound (Table I) is similar to that of the *exo*-COOH nonane, indicating that the stable chair–chair conformation of the nonane is responsible for the observed inhibition. Together with the other data from Table I (see below) these results support the view that the chair–chair backbone provides a good topographical fit to the active site. We therefore conclude that

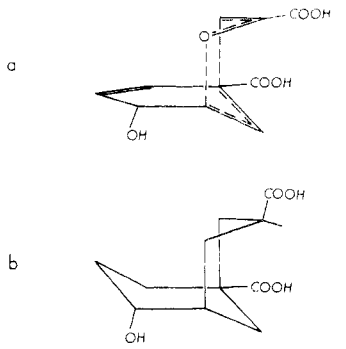

FIGURE 5: Diagrammatic representations of the boat-like alternative for the transition state structure and a stable analogue of this conformation. (a) Boat-like transition state structure; (b) *exo*-6-hydroxybicyclo[3.3.1]-nonane-1,*endo*-3-dicarboxylic acid.

the rearrangement of chorismate to prephenate catalyzed by chorismate mutase–prephenate dehydrogenase proceeds via a chair-like intermediate.

Structure–Activity Relationships. The rate of rearrangement of chorismate to prephenate is enhanced approximately two million-fold by chorismate mutase–prephenate dehydrogenase from *Aerobacter aerogenes* (Andrews et al., 1973), and a perfect transition state analogue could therefore bind the active site some 10^6 times more strongly than chorismate. The inhibitors studied here, although more potent than any previously available, do not approach these levels of inhibition. We have therefore included a series of related structures in order to determine the importance of different molecular fragments in binding to the active site.

The role of the hydrocarbon backbone is illustrated by comparison of the various monosubstituted acids listed in Table 1. In particular, the 400-fold increase in potency on passing from acetic acid to adamantane-1-acetic acid or adamantane-1-carboxylic acid demonstrates the importance of the hydrocarbon skeleton in binding to the enzyme. At 37 °C this decrease in K_I corresponds to a contribution of approximately 3.5 kcal/mol from van der Waals interactions between the adamantane ring and the enzyme, and thus confirms the view that the chair–chair conformation reflects the structure of the active site. In support of the latter conclusion, we have observed no comparable inhibition in any of the monocarboxylic or dicarboxylic acids from acetic to butyric and glutamic to pimelic, respectively.

It is equally clear, however, that the carboxyl group, which is ionized at pH 7.5 in all of the compounds studied, plays a substantial role in binding. This is particularly evident in the increased potency of adamantane-1-carboxylic acid relative to 1-hydroxyadamantane (uncharged) and 1-aminoadamantane (positively charged). It also results in the weak inhibition due to acetic acid.

The significant increase in inhibition accompanying 6-hydroxy substitution of adamantane-1,3-dicarboxylic acid indicates the importance of the hydroxyl group in binding to the active site, and the correct placement of this group is confirmed by the failure of *endo*-6-hydroxybicyclo[3.3.1]nonane-1,*exo*-3-dicarboxylic acid to inhibit the enzyme, in contrast to the corresponding *exo*-6 compound. Both nonanes adopt an identical chair–chair conformation, differing only in stereochemistry around the hydroxyl carbon.

Although adamantane-1-acetic acid and adamantane-1-carboxylic acid are outstanding inhibitors, adamantane-1,3-diacetic acid, adamantane-1,3-dicarboxylic acid, and 1-carboxyadamantane-3-acetic acid are comparatively weak. A possible explanation is that the long partial bonds of the

TABLE II: Intersubstituent Distances in the Alternative Transition State Structures and Their Analogues.

	Intersubstituent distances (Å)		
	Ring carboxyl to side-chain carboxyl[a]	Ring carboxyl to hydroxyl	Side-chain carboxyl to hydroxyl
Chair-like transition state[b]	5.6	5.4	5.4
exo-6-Hydroxybicyclo[3.3.1]nonane-1,*exo*-3-dicarboxylic acid[c]	5.6	5.0	6.1
6-Hydroxyadamantane-1,3-dicarboxylic acid[c]	5.6	5.0	6.1
Boat-like transition state[b]	5.3	5.5	6.3
exo-6-Hydroxybicyclo[3.3.1]nonane-1,*endo*-3-dicarboxylic acid[c]	5.4	5.0	6.5

[a]Designations "ring" and "side chain" refer to corresponding substituents in chorismate or prephenate molecules. [b]From results of MINDO/3 calculations (Andrews and Haddon, in preparation). [c]Calculated using standard geometric parameters (Sutton, 1965).

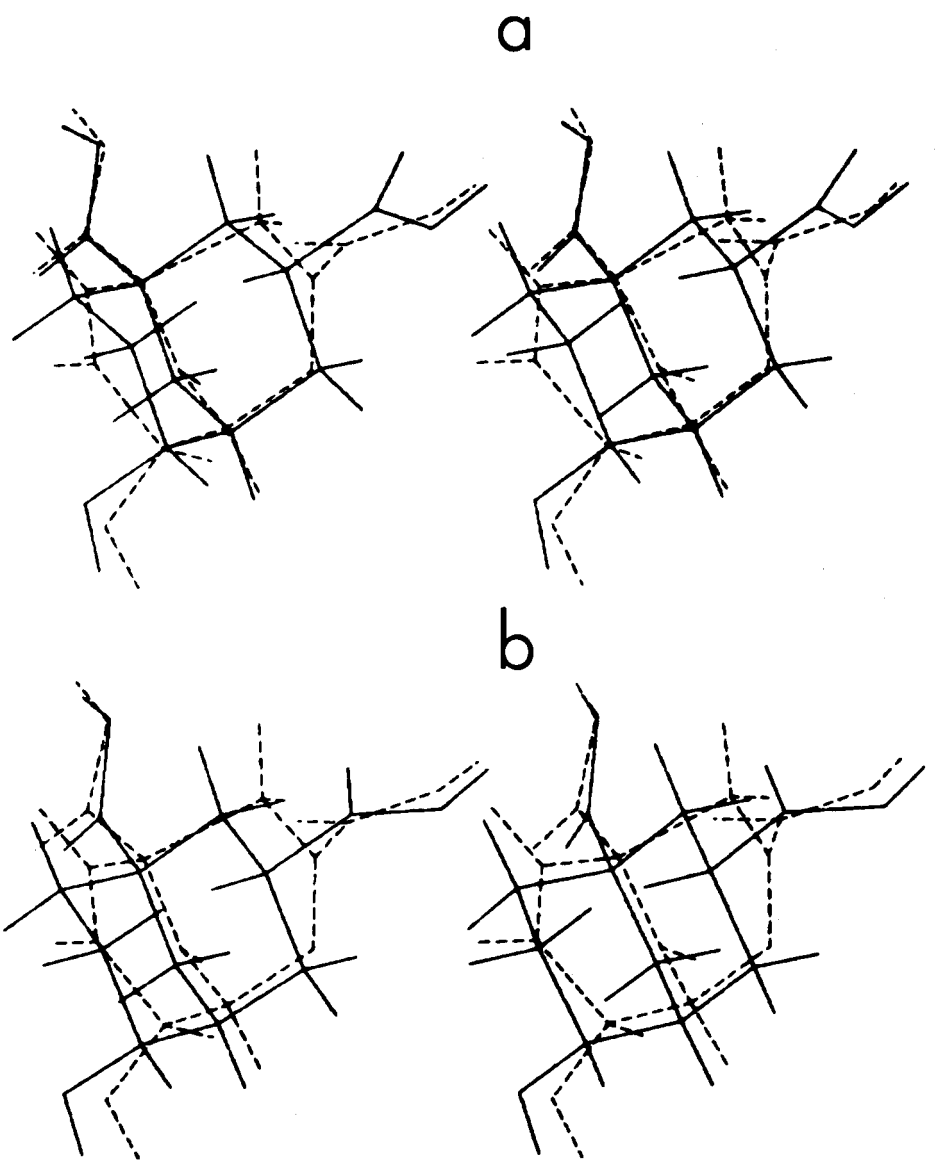

FIGURE 6: Stereoscopic superimpositions of *exo*-6-hydroxybicyclo[3.3.1]nonane-1,*exo*-3-dicarboxylic acid on the chair-like transition state computed by MINDO/3 (Andrews and Haddon, in preparation). (a) Optimum superimposition of ring systems; (b) best superimposition of side-chain carboxyl groups.

transition state are inadequately reproduced in the analogues, particularly in the case of the dicarboxylic compound, but the data in Table II demonstrate that the intersubstituent distances in the analogues are actually rather close to those of the calculated transition state structures. Furthermore, the reduced inhibition which follows introduction of a second acid moiety is indicative of a repulsive interaction. This is difficult to explain on the grounds that the analogues are too small.

The alternative explanation is that the analogues fail to reproduce the orientation of the side-chain carboxyl group with respect to the rest of the molecule. This would be consistent with the improvement in inhibition on passing from adamantane-1,3-dicarboxylic acid to adamantane-1,3-diacetic acid, since the conformational flexibility provided by the additional methylene groups may serve to reduce repulsive interactions. It is also supported by the superimpositions of *exo*-6-hydrox-

ybicyclo[3.3.1]nonane-1,*exo*-3-dicarboxylic acid on the chair transition state structure shown in Figure 6. Both of these superimpositions provide maximum overlap between corresponding atoms in the two structures (average separation 0.20 Å), particularly in the ring carboxyl and hydroxyl groups. It is clear, however, that good superimposition of the hydrocarbon backbone, as in Figure 6a, is incompatible with reasonable placement of the side-chain carboxyl group, as in Figure 6b. Molecules with better alignment of the side-chain carboxyl group are therefore required to obtain maximum inhibition.

Because of the nature of the partial bonds in the transition state, correct alignment of the side-chain carboxyl group may prove to be impossible. Efforts to design better inhibitors are nevertheless warranted, particularly in view of the recent observation (Danilenko et al., 1975) that adamantane-1-carboxylic acid and adamantane-1-acetic acid display broad spectrum bacteriostatic activities at concentrations similar to those found here to inhibit chorismate mutase. It is likely that 4-hydroxyadamantane-1-carboxylic acid, which combines the best features of the present series of inhibitors, but which lacks the second acidic moiety, would provide a sound starting point in the search for better inhibitors.

References

Andrews, P. R., Smith, G. D., and Young, I. G. (1973), *Biochemistry 12,* 3492.

Appleton, R. A., Egan, C., Evans, J. M., Graham, S. H., and Dixon, J. R. (1968), *J. Chem. Soc.,* 1110.

Bott, K. (1968), *Chem. Ber. 101,* 564.

Cain, E. N., and Welling, L. L. (1975), *Tetrahedron Lett.,* 1353.

Danilenko, G. I., Palii, G. K., Mokhort, N. A., and Baklan, V. F. (1975), *Fiziol. Akt. Veshchestva 7,* 144.

Dewar, M. J. S. (1975), *Chem. Br. 11,* 97.

Doering, W. von E., and Roth, W. R. (1962), *Tetrahedron 18,* 67.

Gibson, F., and Pittard, J. (1968), *Bacteriol. Rev. 32,* 465.

Ife, R. J., Ball, L. F., Lowe, P., and Haslam, E. (1976), *J. Chem. Soc., Perkin Trans 1,* 1776.

Koch, G. L. E., Shaw, D. C., and Gibson, F. (1971), *Biochim. Biophys. Acta 229,* 795.

Koch, G. L. E., Shaw, D. C., and Gibson, F. (1972), *Biochim. Biophys. Acta 258,* 719.

Marvell, E. N., and Knutson, R. S. (1970), *J. Org. Chem. 35,* 388.

Schaefer, J. P., and Honig, L. M. (1968), *J. Org. Chem. 33,* 2655.

Stetter, H., Schwarz, M., and Hirschhorn, A. (1959), *Chem. Ber. 92,* 1629.

Sutton, L. E. (1965), *Chem. Soc., Spec. Publ. No. 11 and 18.*

Wolfenden, R. (1976), *Annu. Rev. Biophys. Bioeng. 5,* 271.

Phosphorylation of Nuclear Proteins in Rat Regenerating Liver†

Chi Ching Chen, Berndt B. Bruegger, C. W. Kern, Y. C. Lin,‡ R. M. Halpern, and Roberts A. Smith*

ABSTRACT: In studies of the phosphorylated proteins in rat liver and Walker-256, it was established that the ratio of various fractions of P–N linkages to P–O linkages varies from 0.6 to 3.1. In rat regenerating liver nuclei, the ratio of P–N and P–O varies with time after partial hepatectomy. Using [^{3}H]-lysine and $^{32}P_i$, it is shown that phosphoryllysine forms in some new and, presumably, some preexisting H1 molecules. Using [^{3}H]histidine and $^{32}P_i$, it is shown that phosphohistidine forms exclusively in preexisting H4. The half-life of H4 phosphohistidine appears to be about 2 h.

Two types of phosphorylation are known to occur in histones; one on hydroxy amino acids forming P–O linkages (Ord et al., 1975), and the other on basic amino acids forming P–N linkages (Chen et al., 1974). The study of the P–O linkages (phosphoserine and phosphothreonine) in histones, which are commonly extracted under acidic conditions, has been facilitated by the acid-stable nature of these linkages. This is reflected by the large amount of experimental data collected on P–O linkages in histones (Ord et al., 1975). The P–N linkages, phosphohistidine, phospholysine, and phosphoarginine (Smith et al., 1976; Bruegger, 1977), are acid-labile and have been demonstrated in phosphorylated myelin basic protein and from chromosomal proteins isolated under neutral or basic conditions. This paper attempts to determine the relative contribution of P–O and P–N linkages to the phosphorylation of the nuclear proteins extracted at various time intervals from rat regenerating liver. H1 and H4 that have been isolated from rat regenerating liver have been shown to contain P–N linkages (Chen et al., 1974). A determination of whether these P–N linkages are formed on old, preexisting H1 and H4 or on new, de novo synthesized H1 and H4 during rat liver regeneration is presented. In addition, we also examined the turnover of the P–N linkage in H4 during rat liver regeneration.

Materials and Methods

Chemicals. [^{3}H]Lysine, [^{3}H]histidine, and carrier-free $^{32}P_i$ were purchased from ICN Pharmaceuticals. Trypsin and Pronase were purchased from Calbiochem. Whole histone was obtained from Sigma Chemical Co. Phospholysine and phosphohistidine were prepared as described previously (Chen et al., 1974).

Preparation of Regenerating Rat Liver. Female Sprague-Dawley rats, 250–300 g, underwent partial hepatectomy by

† From the Department of Chemistry and Molecular Biology Institute, University of California, Los Angeles, California 90024. *Received October 19, 1976; revised manuscript received July 5, 1977.* This work was supported by a grant from the United States Public Health Service (CA 13196). Department of Chemistry Publication No. 3722.

‡ Department of Chemistry, National Taiwan University, Taipei, Taiwan, ROC.